

available at www.sciencedirect.comjournal homepage: www.elsevier.com/locate/carbon

Improved field emission properties of double-walled carbon nanotubes decorated with Ru nanoparticles

Chunli Liu^a, Kwang Sub Kim^a, Jihye Baek^b, Youngmi Cho^c, Seungwu Han^b, Soo-Won Kim^a, Nam-Ki Min^d, Youngmin Choi^e, Jong-Ung Kim^e, Cheol Jin Lee^{a,*}

^aSchool of Electrical Engineering, Korea University, Anam-dong, Seongbuk-gu, Seoul 136-713, Republic of Korea

^bDepartment of Physics, Ewha Womans University, Seoul 120-750, Republic of Korea

^cCAE Team, R&D Center, Samsung SDI, Yongin 446-577, Republic of Korea

^dDepartment of Control and Instrumentation Engineering, Korea University, Jochiwon 339-700, Republic of Korea

^eDevice Nano Materials Center, Korea Research Institute of Chemical Technology, Daejeon 305-600, Republic of Korea

ARTICLE INFO

Article history:

Received 5 September 2008

Accepted 27 December 2008

Available online 6 January 2009

ABSTRACT

The field emission properties of double-walled carbon nanotubes (DWCNTs) were remarkably improved by decorating their surface with ruthenium (Ru) metal nanoparticles. The Ru nanoparticles were attached effectively on the surface of DWCNTs via a chemical procedure. The Ru-decorated DWCNTs showed lower turn-on voltage, higher emission current density, and improved emission uniformity compared with pristine DWCNTs. The effect of Ru nanoparticles on the work function and density of states was evaluated by the first-principles calculation. The enhanced field emission properties of Ru-DWCNTs were mainly attributed to the Ru nanoparticles which increased the field enhancement factor and the density of emission sites. Our results indicate that the Ru-decorated DWCNTs can be used as an effective field emitter for various field emission devices.

© 2009 Elsevier Ltd. All rights reserved.

1. Introduction

Electron field emission from carbon nanotubes (CNTs) has been studied extensively since the discovery of CNTs was reported in 1991 [1–5]. Due to the high-aspect ratio, excellent electrical property, and good mechanical stiffness, CNTs has been considered as an ideal candidate for various field emission applications such as lamps and flat panel display devices [6,7], X-ray tubes [8,9], vacuum gauges [10], and microwave amplifiers [11]. For practical CNT-based field emission devices, it is necessary to improve the emission current density, uniformity, and stability. To achieve high emission performance from CNT emitters, various methods such as surface treatment of the CNT emitters [12–14], doping of CNTs with nitrogen [15,16], and utilizing vertical aligned CNT arrays [17] have been studied. Among these var-

ious techniques, coating the surface of CNTs with other materials has been studied as one candidate to improve field emission properties. The CNTs coated with low work function materials such as LaB₆, Cs, or Hf showed lower turn-on field than that of the pristine CNTs [18–20]. Moreover, CNTs coated with nanoparticles such as RuO₂, ZnO, and Ti nanoparticles also indicated improved field emission properties [21–25]. Recently, CNTs coated with ruthenium (Ru) nanoparticles showed enhanced catalytic effect due to high density active sites [26–28]. Ru nanoparticles can be easily coated onto CNTs via chemical methods, and Ru is more stable than the low work function alkali metals when exposed to oxygen. Moreover, the melting point of Ru (2607 °C) is much higher than that of RuO₂ (1200 °C). Therefore, it would be interesting to investigate the field emission properties of Ru-coated CNTs.

* Corresponding author. Fax: +82 2 921 4722.

E-mail address: cjlee@korea.ac.kr (C.J. Lee).

0008-6223/\$ - see front matter © 2009 Elsevier Ltd. All rights reserved.

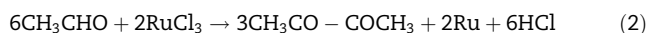
doi:10.1016/j.carbon.2008.12.054

In this work, we report the effect of Ru nanoparticle coating on the improved field emission properties of double-walled CNTs (DWCNTs). We also explain the enhanced field emission properties of Ru nanoparticles-coated DWCNTs (Ru-DWCNTs) using first-principles calculations of the work function and the density of states (DOS).

2. Experimental

2.1. Coating of Ru nanoparticles on DWCNTs

The coating of Ru nanoparticles onto the DWCNTs was performed using the following procedure. First, 0.0182 g of DWCNTs were added to a solution of polyvinylpyrrolidone (PVP) (Aldrich, MW 10,000) in 10 mL ethylene glycol (Aldrich, anhydrous 98%), and dispersed by ultrasonication for 30 min. Then, 3.2×10^{-4} mole of RuCl_3 (mole ratio of PVP/ $\text{RuCl}_3 = 0.02$) was added to the dispersed solution, which was then stirred at 180 °C for 1 h, followed by rapid cooling to room temperature and ultrasonication for 30 min. During this process, RuCl_3 was reduced to Ru as described by the chemical Eqs. (1) and (2). After the above procedure, in order to remove residual impurities, acetone was added to the solution and was dispersed by a centrifugal separator at 17,000 rpm for 15 min. The same process was repeated once using distilled water instead of acetone. Finally, the resulting solution was freeze-dried to obtain Ru-DWCNTs.



The microstructure of DWCNTs before and after Ru coating was characterized by high-resolution transmission electron microscopy (HRTEM). The chemical state of the nanoparticles was further characterized by X-ray photoelectron spectra (XPS) and X-ray diffraction (XRD). To investigate the effect of the coating procedure on the structure of the DWCNTs, microscopic Raman scattering was carried out at room temperature using Ar^+ laser excitation at a wavelength of $\lambda_{\text{el}} = 514.5$ nm.

2.2. Measurement of field emission properties

The field emission measurements were performed in a vacuum chamber at 1×10^{-7} Torr using the diode configuration. The field emitters using Ru-DWCNTs were fabricated by the following method. Firstly, Ag paste about 50 μm -thick was pasted on the 1×1 cm^2 Ti (200 nm)/Cr (300 nm)/*n*-Si substrates. While the Ag paste was still wet, the Ru-DWCNTs or pristine DWCNTs were deposited on the substrate through a mesh with holes of 30 μm . In this way, the CNTs can be distributed uniformly on the substrate. The thickness of the DWCNT films on the Ag paste is about 30 μm . The substrate deposited with DWCNTs was then dried in air for 30 min and then baked at 80 °C for 20 min in order to obtain good mechanical adhesion and ohmic contact between the DWCNTs and the substrate. The anode was a piece of cylinder-shaped stainless steel with a diameter of 5 mm. The gap between the cathode and the anode was 270 μm . Fig. 1 shows

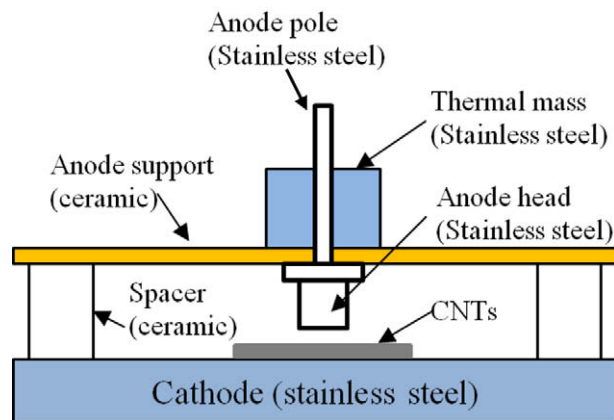


Fig. 1 – Schematic of field emission measurement setup.

the detailed schematic of the apparatus of field emission measurement. To evaluate the emission uniformity, a phosphor-coated indium-tin-oxide/glass substrate was used as an anode to observe the light emission patterns.

3. Results and discussion

3.1. Physical properties of Ru-DWCNTs

We used HRTEM to characterize the microstructure of Ru-DWCNTs. Fig. 2a shows the HRTEM image taken from the pristine DWCNTs. The inset of Fig. 2a clearly shows that two CNTs have two graphene layers and reveals that the DWCNTs have diameters about 5 nm. After the Ru coating process, the DWCNTs were found to be decorated with quite uniform-sized particles on their outer surfaces, as shown in Fig. 2b and c. It is considered that the Ru nanoparticles may be selectively attached on the defect sites of the CNTs [29]. In the inset of Fig. 2c, the selected area electron diffraction (SAED) of these Ru nanoparticles presents characteristic diffraction circles of metallic Ru. The concentric rings shown in the diffraction pattern indicate that the metallic Ru nanoparticles are composed of fine crystallites and are oriented randomly on the CNT surface [27]. The size distribution of the Ru nanoparticles is summarized in Fig. 2d, showing that the diameters of most of the nanoparticles are about 2.2 nm. From TEM observations in Fig. 2a and c, we can suggest that there is no significant change in the structure of DWCNTs after the Ru coating process.

XPS and XRD measurements were performed to characterize the chemical state of the nanoparticles. Fig. 3a shows the Ru 3p region of the XPS spectrum from the Ru-DWCNTs. The binding energies of Ru 3p_{3/2} at 461.0 eV and Ru 3p_{1/2} at 483.2 eV correspond to the photoemission from metallic Ru [30]. Additionally, the major diffraction peaks from nanoparticles were observed in the X-ray powder diffraction 2 θ scan, as shown in Fig. 3b. The peaks at 44.0°, 38.4°, and 42.2° correspond to the typical crystal faces (101), (100), and (002) of metallic Ru. Therefore, the nanoparticles on the outer surfaces of the DWCNTs are clearly confirmed to be metallic Ru.

The Raman spectra from the DWCNTs before and after the Ru decoration process are shown in Fig. 4. The Raman spectra

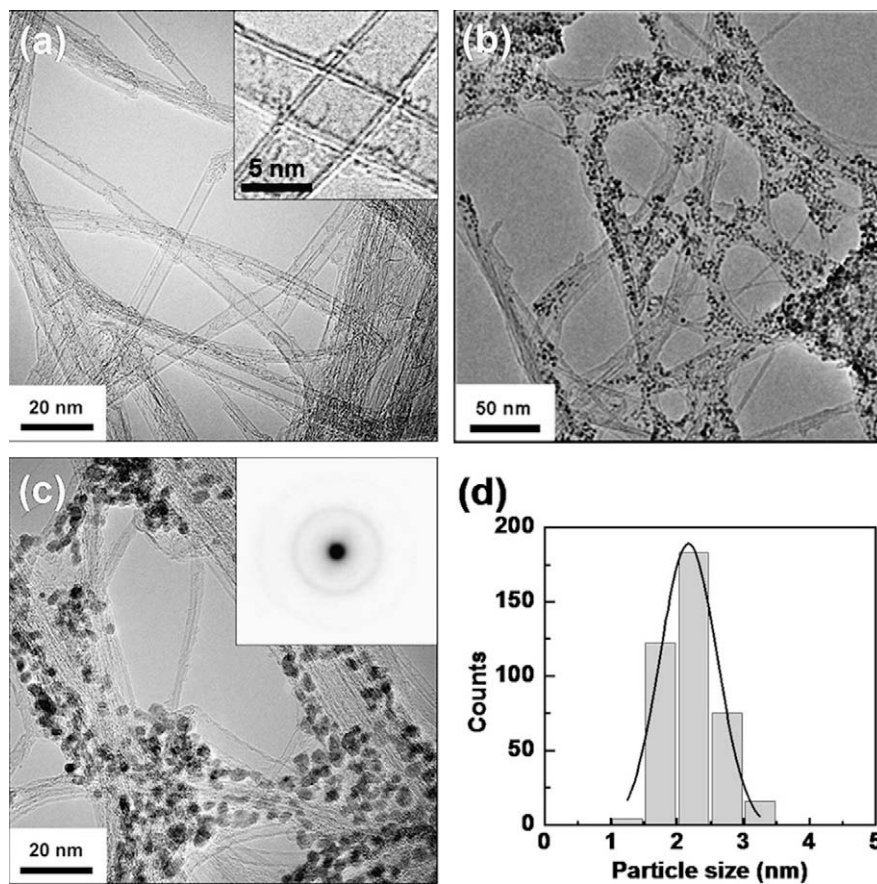


Fig. 2 – HRTEM image of DWCNTs. (a) Before Ru coating; (b) and (c) after Ru coating. The inset in (c) shows the SAED of the Ru nanoparticles; (d) shows the size distribution of the Ru nanoparticles on DWCNTs.

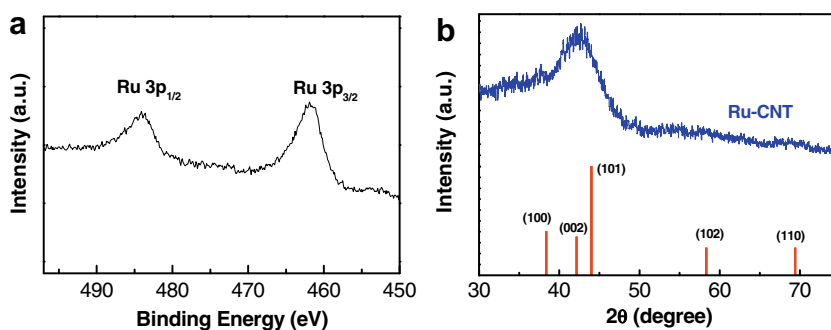


Fig. 3 – XPS spectrum and XRD pattern of the Ru-DWCNTs: (a) Ru 3p region of the XPS spectrum; (b) XRD pattern, indicating the peaks from metallic Ru.

show a very similar peak arrangement regardless of Ru decoration on the surface of DWCNTs, consisting of the radial breathing mode (RBM) at $100\text{--}300\text{ cm}^{-1}$, the G-band around 1580 cm^{-1} , and the D-band around 1350 cm^{-1} . The inset of Fig. 4 shows a magnified Raman spectrum in the low frequency region of $100\text{--}300\text{ cm}^{-1}$. The RBMs exhibit several peak components, which is a typical characteristic of DWCNTs [31]. Despite the decoration of Ru nanoparticles on the surface of DWCNTs, the Raman spectrum shows an intensity ratio of I_G/I_D about 15, indicating a low defect level in the graphene structure of DWCNTs. The similarity between the

Raman spectra patterns from the two kinds of DWCNTs, especially the full width half-maximum of D-band and G-band peaks, implies that the Ru coating process induces no significant damage to the crystalline structure of DWCNTs.

3.2. Field emission properties of Ru-DWCNTs

Fig. 5a shows dramatically improved field emission from the Ru-DWCNTs. As compared with the pristine DWCNTs, the turn-on electric field (E_{to}) of Ru-DWCNTs corresponding to $10\text{ }\mu\text{A}/\text{cm}^2$ is lowered from 2.5 to 1.3 $\text{V}/\mu\text{m}$, and the thresh-

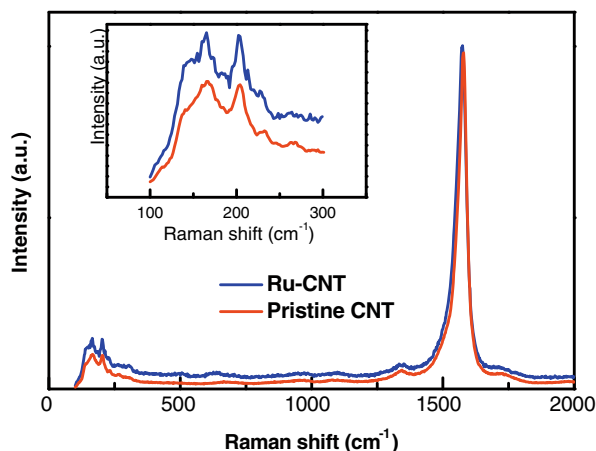


Fig. 4 – Raman spectra taken from the DWCNTs before and after Ru coating. The inset is the magnified RBM peak structure of Raman spectra in the range of 100–300 cm^{-1} .

old electric field (E_{th}) corresponding to 1 mA/cm^2 is decreased from 6.5 to 3.9 $\text{V}/\mu\text{m}$. The values of E_{to} and E_{th} from DWCNT emitters are quite diverse in the literature due to the different

synthesis techniques of DWCNTs and emitter structures. The typical range of E_{to} and E_{th} for DWCNTs are 1–2 and 1.7–5 $\text{V}/\mu\text{m}$, respectively [32,33]. In this study, the decoration of Ru nanoparticles effectively lowered E_{to} and E_{th} of DWCNTs, and their values from Ru-DWCNTs are relatively low as compared to the reported values from other DWCNTs. Regarding the dependence of coating materials, up to now there has been no report related to coated-DWCNTs. For MWCNT thin film field emitters, SiO_2 - and MgO -coated MWCNTs showed E_{to} of 2.7 $\text{V}/\mu\text{m}$ and 4.8 $\text{V}/\mu\text{m}$, respectively [34]; Hf-coated CNTs showed E_{th} of 3.1 $\text{V}/\mu\text{m}$ [20]. Therefore, our Ru-DWCNTs field emitters can be operated at similar or lower electric field as compared with other coated-CNTs.

The corresponding Fowler–Nordheim (F–N) plots of the I–V curves are shown in the inset of Fig 5, where the straight lines indicate the field emission characteristics. The semi-logarithmic form of the F–N equation is expressed as:

$$\ln(J/F^2) = \ln(a\beta^2/\phi) - (b\phi^{3/2}/\beta)(1/F) \quad (3)$$

where J is the current density, $a = 1.54 \times 10^{-6}$ ($\text{A V}^{-2} \text{eV}$), $b = 6.83 \times 10^9$ ($\text{eV}^{-3/2} \text{V m}^{-1}$), β is the field enhancement factor, ϕ is the work function of the emitter, and F is the applied macroscopic electric field. According to Eq. (3), if we assume

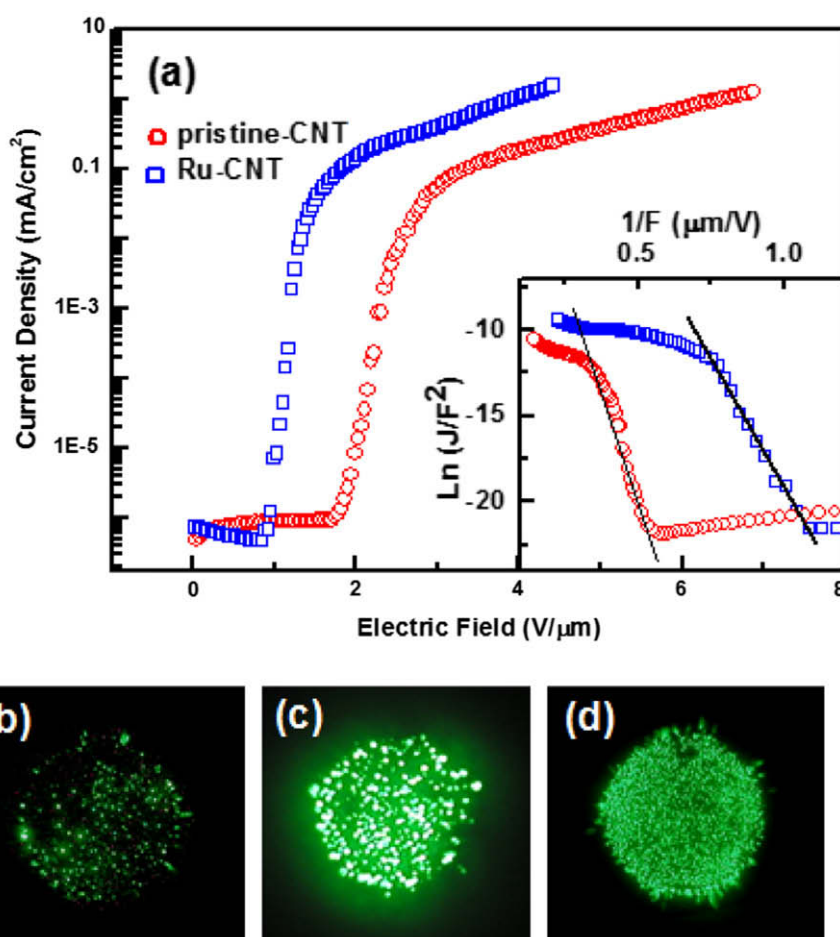


Fig. 5 – (a) The field emission I–V characteristic of DWCNTs with and without Ru nanoparticle coating. The inset shows the F–N plots, with the slope indicated by the straight line. Emission patterns from (b) pristine DWCNTs with 0.05 mA/cm^2 @ 2.96 $\text{V}/\mu\text{m}$, (c) pristine DWCNTs with 0.4 mA/cm^2 @ 5 $\text{V}/\mu\text{m}$, and (d) Ru-CNTs with 0.4 mA/cm^2 @ 2.96 $\text{V}/\mu\text{m}$. The diameter of the CNT cathode was 15 mm.

the work function of the DWCNT to be 4.5 eV, the field enhancement factor calculated from the slope of the F–N plot is 1349 and 2231 for the pristine DWCNTs and Ru-DWCNTs, respectively. In this work, it is considered that the difference in morphology between the two kinds of DWCNTs is not significant because we fabricated the DWCNT emitters using the same fabrication process. Thus, it is suggested that the enhanced field emission properties of Ru-DWCNTs are mainly attributed to the Ru nanoparticles on the surface of DWCNTs. It is noteworthy that the field enhancement factor of Ru-DWCNTs can be higher due to the increased aspect ratio as compared with the pristine DWCNTs.

In addition to the improved field emission I–V characteristics, better emission uniformity is observed from the emission pattern of the Ru-DWCNT emitter, as shown in Fig. 5d. As compared with the emission pattern of pristine DWCNT (shown in Fig. 5b) at same applied field of 2.96 V/ μm , it is obvious in Fig. 5d that the density of field emission sites increased after Ru nanoparticle coating. Similarly, at same emission current density of 0.4 mA/cm², the Ru-DWCNT emitter also has higher density of emission sites than the pristine DWCNTs (shown in Fig. 5c). The estimated emission site density from the Ru-DWCNT emitter is about $1.5 \times 10^3/\text{cm}^2$, which is comparable to the high emission site density from a well treated uniform CNT emitter [35]. The increased emission sites are mainly caused by the Ru nanoparticles-coated on the surface of DWCNTs.

We also compared the emission stability of Ru-DWCNTs with that of pristine DWCNTs at 1 mA/cm² under dc voltage supply for 20 h. If the lifetime is defined as a time span to reach the half of the initial current density, the lifetime of Ru-CNTs is about 20 h as compared with 10 h from the pristine CNTs. We also tested several emitters made from each type of CNTs, and the results are similar. It should be noted that the lifetime measurement was performed under dc voltage supply, which is much sever than the pulsed voltage conditions used by several other groups. Although, the Ru-CNTs studied in this work still shows degradation over long time operation, it is acceptable to real application of field emission devices. In this work, we can confirm obviously increased

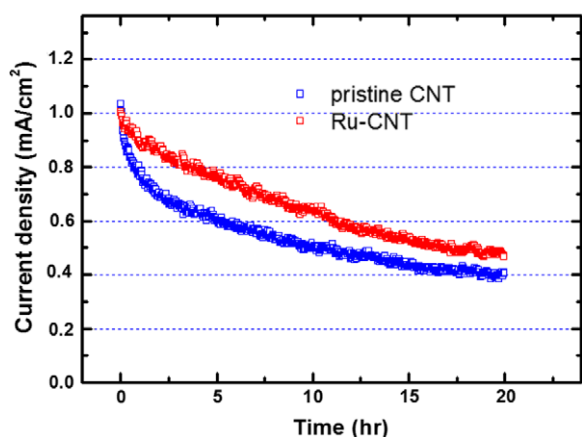


Fig. 6 – Lifetime comparison between pristine CNTs and Ru-CNTs. Measurements are performed at 1 mA/cm² under dc voltage for 20 h.

emission stability from the Ru-CNT emitter compared with the pristine CNT emitter as shown in Fig. 6. The elongated lifetime of the Ru-CNT emitters is considered due to the protection effect of Ru nanoparticles against oxygens since they prefer to attach on the defect sites of CNT sidewalls. It is expected that with further optimization of the coating process and Ru nanoparticles density on the surface of CNTs, the field emission performance of Ru-CNTs can be further improved.

3.3. First-principles calculations

To investigate the microscopic origin for the enhanced field emission from Ru-DWCNTs, we carried out the first-principles calculations using the VASP code [36,37]. First, we investigated the DOS near Fermi level when Ru atoms are attached on a (5,5) CNT, and the results are shown in Fig. 7. For a realistic description of the field emission, we applied an electric field of 5 V/nm and used localized atomic orbitals [25]. It is obvious that the DOS is significantly increased when Ru atoms are attached. This implies that Ru particles can encourage field emission when they are present on the DWCNTs. This result agrees well with the lower turn-on voltage and the higher density of emission sites from Ru-DWCNTs as shown in Fig. 5a and d.

Next, the change of work function was examined as the Ru particles were attached to the sidewall of (5,5) CNT, as shown in Fig. 8. Because of periodic boundary conditions employed in the calculation, the Ru particles are repeated every three unit cells. From a comparison of total energies at various positions, it was found that the Ru atom is most stable when it is above the center of the hexagon, as in Fig. 8a. In Fig. 8a and c, either a Ru atom or a Ru₄ cluster is attached to every three unit cells, whereas four Ru atoms are attached in Fig. 8b. In this way, we examined the effect of the size of Ru particle (Fig. 8a and c) and the density of Ru particle (Fig. 8a and b) on the work function. The work function for these model structures is summarized in Table 1. It is seen that the work function is lowered due to the charge transfer between the CNT and the Ru atoms or clusters. We note that if the change in the slope of F–N plot shown in Fig. 5a is only due to a lowered work function, the work function of Ru-

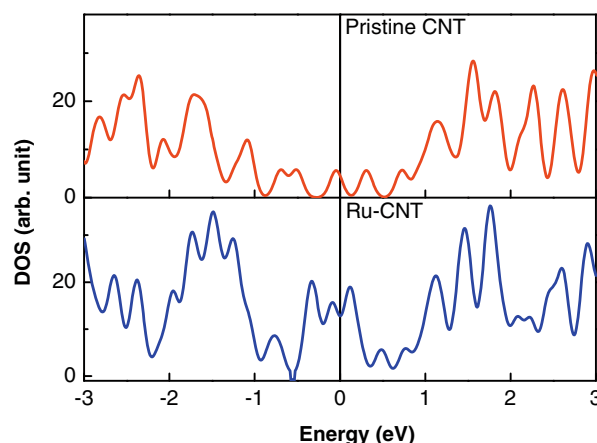


Fig. 7 – The DOS for pristine and Ru-CNTs under the external electric field of 5 V/nm.

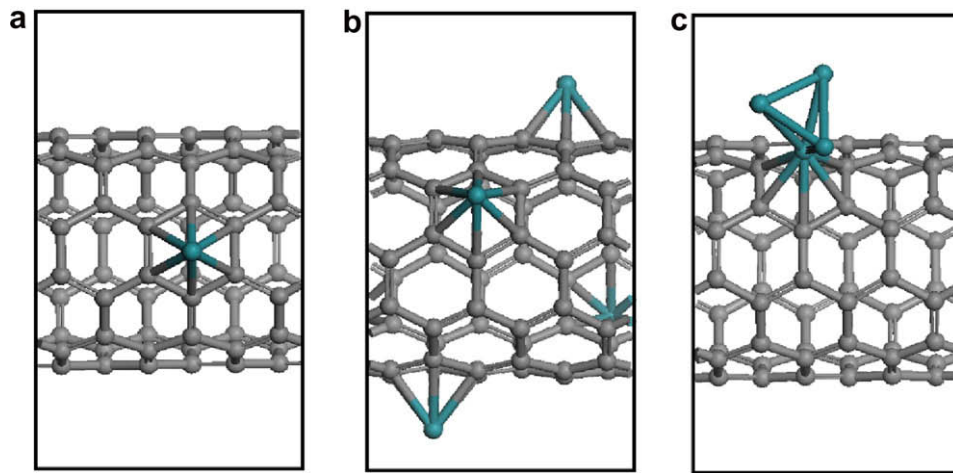


Fig. 8 – The unit cell of a (5,5) CNT with the Ru attachment types. (a) One and (b) four Ru atoms are attached. (c) A Ru₄ cluster is adsorbed.

Table 1 – The work function for model structures in Fig. 8.

Adsorption type	Clean	Ru	4Ru	Ru ₄
Work function (eV)	4.48	4.02	3.53	4.04

DWCNTs calculated using Eq. (3) should be about 3.2 eV, which is lower than the predicted values (4.02 or 3.53 eV) shown in Table 1. This suggests that besides the work function, other parameter like the field enhancement factor β may influence field emission from Ru-DWCNTs, which can be understood from the increased DOS as calculated above. Therefore, we suggest that the enhanced field emission properties of Ru-DWCNTs are mainly attributed to the increased field enhancement factor besides lower work function.

4. Conclusions

We decorated the outer surface of DWCNTs with metallic Ru nanoparticles using a chemical method, and studied their field emission properties. We found that Ru nanoparticles can dramatically enhance the field emission performance from DWCNTs. Both turn-on field and threshold field were largely decreased due to the decoration of Ru nanoparticles on the surface of DWCNTs. The enhanced emission stability of the Ru-CNT emitters is considered due to the protection effect of Ru nanoparticles against oxygens because they prefer to attach on the defect sites of CNT sidewalls. According to first-principles calculations, Ru nanoparticles on DWCNTs could lower work function and increase the DOS near Fermi level. It is considered that the enhanced field emission properties of Ru-DWCNTs were mainly caused by increased field enhancement factor besides lower work function.

Acknowledgments

This work was supported by the Korea Science and Engineering Foundation (KOSEF) NRL Program grant funded by the Korea government (MEST) (No. R0A-2008-000-20071-0) and supported by MOCIE of Energy of Korea through a Compo-

nents and Materials Technology Development project (No. 5052-DG2-0081) and supported by the Korea Foundation for International Cooperation of Science and Technology (KICOS) through a grant provided by the MOST in K20601000002-07E0100-00220. This work was also supported by the Korea Basic Science Institute.

REFERENCES

- [1] Rinzler AG, Hafner JH, Nikolaev P, Lou L, Kim SG, Tomanek D, et al. Unraveling nanotubes-field emission from an atomic wire. *Science* 1995;269(5230):1550–3.
- [2] de Heer WA, Châtelain A, Ugarte D. A carbon nanotube field emission electron source. *Science* 1995;270(5239):1179–80.
- [3] Saito Y, Hamaguchi K, Hata K, Uchida K, Tasaka Y, Ikazaki F, et al. Conical beams from open nanotubes source. *Nature* 1997;389(6651):554–5.
- [4] Lee CJ, Kim DW, Lee TJ, Choi YC, Park YS, Lee YH, et al. Synthesis of aligned carbon nanotubes using thermal chemical vapor deposition. *Chem Phys Lett* 1999;312(5–6):461–5.
- [5] Bonard JM, Salvetat JP, Stockli T, Forro L, Chatelain A. Field emission from carbon nanotubes: perspectives for applications and clues to the emission mechanism. *Appl Phys A* 1999;69(3):245–54.
- [6] Choi WB, Chung DS, Kang JH, Kim HY, Jin YW, Han IT, et al. Fully sealed, high-brightness carbon nanotube field emission display. *Appl Phys Lett* 1999;75(20):3129–31.
- [7] Saito Y, Uemura S. Field emission from carbon nanotubes and its application to electron sources. *Carbon* 2000;38(2):169–82.
- [8] Yue GZ, Qiu Q, Gao B, Cheng Y, Zhang J, Shimoda H, et al. Generation of continuous and pulsed diagnostic imaging x-ray radiation using a carbon nanotube-based field emission cathode. *Appl Phys Lett* 2002;81(2):355–7.
- [9] Sugie H, Tanemura M, Filip V, Iwata K, Takahashi K, Okuyama F. Carbon nanotubes as electron source in an x-ray tube. *Appl Phys Lett* 2001;78(17):2578–80.
- [10] Cho B, Itagaki T, Ishikawa T, Oshima C. Measurement of pressures in 10–10 Pa range from the damping speed of field emission current. *Appl Phys Lett* 2007;91(1):012105-1–3.
- [11] Teo KBK, Minoux E, Hudanski L, Peauger F, Schnell JP, Gangloff L, et al. Microwave devices – carbon nanotubes as cold cathodes. *Nature* 2005;437(7061):968.

- [12] Kim DH, Kim CD, Lee HR. Effects of the ion irradiation of screen-printed carbon nanotubes for use in field emission display applications. *Carbon* 2004;42(8–9):1807–12.
- [13] Zhu YW, Cheong FC, Yu T, Xu XJ, Lim CT, Thong JTL, et al. Effects of CF_4 plasma on the field emission properties of aligned multi-wall carbon nanotube films. *Carbon* 2005;43(2):395–400.
- [14] Jin F, Liu Y, Day CM, Little SA. Enhanced electron emission from functionalized carbon nanotubes with a barium strontium oxide coating produced by magnetron sputtering. *Carbon* 2007;45(3):587–93.
- [15] Stephan O, Ajayan PM, Colliex C, Redlich Ph, Lambert JM, Bernier P, et al. Doping graphitic and carbon nanotube structures with boron and nitrogen. *Science* 1994;266(5):1683–5.
- [16] Golberg D, Bando Y, Bourgeois L, Kurashima K, Sato T. Large-scale synthesis and HRTEM analysis of single-walled B- and N-doped carbon nanotube bundles. *Carbon* 2000;38(14):2017–27.
- [17] Bonard JM, Croci M, Klinker C, Kurt R, Noury O, Weiss N. Carbon nanotube films as electron field emitters. *Carbon* 2002;40(10):1715–28.
- [18] Wei W, Jiang K, Wei Y, Liu P, Liu K, Zhang L, et al. LaB_6 tip-modified multi-walled carbon nanotube as high quality field emission electron source. *Appl Phys Lett* 2006;89(20):203112-1-3.
- [19] Wadhawan A, Stallcup II RE, Perez JM. Effects of Cs deposition on the field emission properties of single-walled carbon nanotube bundles. *Appl Phys Lett* 2001;78(1):108–10.
- [20] Zhang JH, Yang CR, Wang YJ, Feng T, Yu WD, Jiang J, et al. Improvement of the field emission of carbon nanotubes by hafnium coating and annealing. *Nanotechnology* 2006;17(1):257–60.
- [21] Noguchi T, Muto H, Tatenuma K, Liu P, Arai F, Fukuda T, et al. Ultrahigh electron emissive carbon nanotubes impregnated with subnano RuO_2 clusters. In: Proceedings of the 5th IEEE conference on nanotechnology, (Nagoya, Japan); 2005.
- [22] Arai F, Liu P, Dong LX, Fukuda T, Noguchi T, Tatenuma K. Pure metal deposit using multi-walled carbon nanotubes decorated with ruthenium dioxide super-nanoparticles. In: Proceedings of the 4th IEEE conference on nanotechnology, (Munich, Germany); 2004. p. 196–8.
- [23] Green JM, Dong L, Gutu T, Jiao J, Conley Jr JF, Ono Y. ZnO-nanoparticle-coated carbon nanotubes demonstrating enhanced electron field emission properties. *J Appl Phys* 2006;99(9):094308-1-4.
- [24] Min YS, Bae EJ, Park JB, Kim UJ, Park WJ, Song JW, et al. ZnO nanoparticle growth on single-walled carbon nanotubes by atomic layer deposition and a consequent lifetime elongation of nanotube field emission. *Appl Phys Lett* 2007;90(26):263104-1-3.
- [25] Cho YM, Kim CW, Moon HS, Choi HM, Park SH, Lee CK, et al. Electronic structure tailoring and selective adsorption mechanism of metal-coated nanotubes. *Nano Lett* 2008;8(1):81–6.
- [26] Planeix JM, Coustel N, Coq B, Brotons V, Kumbhar PS, Dutartre R, et al. Application of carbon nanotubes as supports in heterogeneous catalysis. *J Am Chem Soc* 1994;116(17):7935–6.
- [27] Sun Z, Liu Z, Han B, Wang Y, Du J, Xie Z, et al. Fabrication of ruthenium-carbon nanotube nanocomposites in supercritical water. *Adv Mater* 2005;17(7):928–31.
- [28] Lu J. Effect of surface modifications on the decoration of multi-walled carbon nanotubes with ruthenium nanoparticles. *Carbon* 2007;45(8):1599–605.
- [29] Li X, Niu J, Zhang J, Li H, Liu Z. Labeling the defects of single-walled carbon nanotubes using titanium dioxide nanoparticles. *J Phys Chem B* 2003;107(11):2453–8.
- [30] Kotz R, Lewerenz HJ, Stucki S. XPS studies of oxygen evolution on Ru and RuO_2 anodes. *J Electrochem Soc* 1983;130(4):825–9.
- [31] Kim SY, Lee JY, Park J, Park CJ, Lee CJ, Shin HJ. Synchrotron X-ray photoelectron spectroscopy and field emission of double-walled carbon nanotubes – dependence on growth temperature. *Chem Phys Lett* 2006;420(4–6):271–6.
- [32] Jung SI, Jo SH, Moon HS, Kim JM, Zang DS, Lee CJ. Improved crystallinity of double-walled carbon nanotubes after a high-temperature thermal annealing and their enhanced field emission properties. *J Phys Chem C* 2007;111(11):4175–9.
- [33] Chen G, Shin DH, Iwasaki T, Kawarada H, Lee CJ. Enhanced field emission properties of vertically aligned double-walled carbon nanotube arrays. *Nanotechnology* 2008;19(41):415703-1-6.
- [34] Yi WK, Jeong TW, Yu SG, Heo JN, Lee CS, Lee JH, et al. Field emission characteristics from wide-bandgap material-coated carbon nanotubes. *Adv Mater* 2002;14(20):1464–8.
- [35] Liang XH, Deng SZ, Xu NS, Chen J, Huang NY, She JC. On achieving better uniform carbon nanotube field emission by electrical treatment and the underlying mechanism. *Appl Phys Lett* 2006;88(11):111501-1-3.
- [36] Kresse G, Hafner J. Abinitio molecular-dynamics for liquid-metals. *Phys Rev B* 1993;47(1):558–61.
- [37] Kresse G, Hafner J. Abinitio molecular-dynamics simulation of the liquid-metal amorphous-semiconductor transition in germanium. *Phys Rev B* 1994;49(20):14251–69.